ISSN 1392–1207. MECHANIKA. 2020 Volume 26(1): 12–17

Experimental study on Mode I fracture of cracked straight through the square specimen (CSTSS)

Lijuan ZHANG*, Zhi WANG, Long LI*****

**School of Mechanics and Engineering Science, Zhengzhou University, Zhengzhou 450001, China, E-mail: zhanglj0526@zzu.edu.cn*

***School of Mechanics and Engineering Science, Zhengzhou University, Zhengzhou 450001, China, E-mail: wangzhi@zzu.edu.cn (Corresponding Author)*

****School of Mechanics and Engineering Science, Zhengzhou University, Zhengzhou 450001, China, E-mail: lilong@gs.zzu.edu.cn*

crossref http://dx.doi.org/10.5755/j01.mech.26.1.22972

1. Introduction

A new type of rock fracture toughness specimen, cracked chevron notched Brazilian disc (CCNBD) was proposed by the International Society for Rock Mechanics, ISRM, in 1995 [1]. Before the method was proposed, a lot of pre-researches had been carried out and the calibration result and stress intensity factor of CCNBD were obtained [2-3]. Because of the difficulty in processing precision of CCNBD, a cracked straight through Brazilian disc (CSTBD) was proposed to determine the fracture toughness of rock [4-5]. And then, the CSTBD was widely used to study the dynamic and static fracture toughness of rock and some useful consequences were gained [6-9]. It was suggested that the test of CSTBD was an effective method to determine the Mode I fracture toughness of rock.

There were also many types of research on the split experiment of square specimens instead of Brazilian disc. And some calculation formulas of tensile strength were given according to the engineering experience [10-12]. There was still a discussion on the stress distribution and failure mechanism of square specimens under splitting load. In the pre-research of this paper, the tensile stress distribution function of the rectangular specimen under splitting load was derived based on Fourier Series Solution. The maximum tensile stress was showed at a certain point in the specimen's symmetry axis and the damage initiated because the maximum tensile stress reaching its tensile strength. The splitting tensile strength formula of rock with a rectangular specimen was established [13-14]. According to the stress distribution of the uncracked square specimen, the stress intensity factor of cracked straight through square specimen (CSTSS) will be established and the shape function will be calibrated through FEM in this paper.

2. Theoretical formula

For a rectangular specimen with a length of $2a$, the width of $2b$, and a thickness of t under a pair of splitting loading q (Fig. 1), the load distribution can be described according to Fourier Series stress calculation theory [13-14].

This is an example of an equation:

$$\frac{q}{q} = A + A\sin\frac{m\pi x}{a} + A\cos\frac{m\pi x}{a}. \tag{1}$$

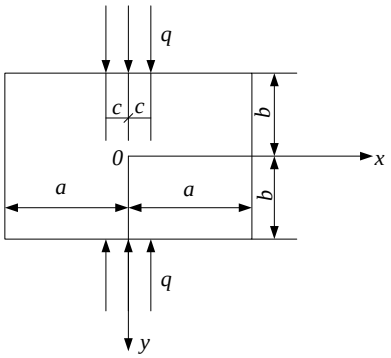

Fig. 1 Schematic diagram of plane force

The actual load can be supposed as:

$$\frac{q}{q} = \begin{cases} 0, -c > x \quad or \quad x > c \\ q, -c \le x \le c \end{cases}. \tag{2}$$

The load can be expanded into the form of Fourier Series:

$$\frac{q}{q} = \frac{qc}{a} + \frac{2q\sin\frac{m\pi c}{a}}{m\pi}\cos\frac{m\pi x}{a}. \tag{3}$$

Where q_u and q_l are upper and lower boundary load, q is cushion block load, $2c$ is the width of the cushion block, $2b$ and $2a$ are the height and length of the specimen, m is an arbitrary positive integer.

When $2c$ is close to 0, the distributed load is reduced to concentrated force:

$$\frac{q}{q} = \frac{qc}{a} + \frac{2qc}{a}\cos\frac{m\pi x}{a}. \tag{4}$$

The general form of the solution of the stress by Fourier Series method is:

$$\sigma = 2A\frac{(\alpha b\cdot\cosh\alpha b)\cosh\alpha y}{\sinh 2\alpha b + 2\alpha b}\sin\alpha x - \\ -\frac{\alpha y\sinh\alpha y\sinh\alpha b}{\sinh 2\alpha b + 2\alpha b}\sin\alpha x. \tag{5}$$

$$\sigma = -2A\frac{(\alpha b\cdot cosh\alpha b + sinh\alpha b)\cosh\alpha y}{sinh2\alpha b + 2\alpha b}sin\alpha x + \\ +2A\frac{\alpha y sinh\alpha y sinh\alpha b}{sinh2\alpha b + 2\alpha b}sin\alpha x, \quad (6)$$

$$\tau = -2A\frac{(\alpha b\cdot cosh\alpha b)sinh\alpha y}{sinh2\alpha b + 2\alpha b}cos\alpha x + \\ +2A\frac{\alpha y cosh\alpha y sinh\alpha b}{sinh2\alpha b + 2\alpha b}cos\alpha x, \quad (7)$$

where: $\alpha = \frac{m\pi}{a}$.The normal stress of any position within the specimen can be calculated through the Eq. (4-7):

$$\sigma = \frac{2P}{at}\frac{(\alpha b\cdot cosh\alpha b - sinh\alpha b)cosh\alpha y\cdot cosax}{sinh2\alpha b + 2\alpha b} - \\ -\frac{2P}{at}\frac{\alpha y sinhay sinhab}{sinh2\alpha b + 2\alpha b}cosax. \quad (8)$$

The normal stress of rectangular specimen under splitting load can be determined by Eq. (6) and the normal stress on the axis of symmetry can be expressed as [13]:

$$\sigma = \frac{2P}{bt}\varphi(y/b), \quad (9)$$

where: $\varphi(y/b)$ is shape factor and

$$\varphi(y/b) = \frac{(\alpha b\cdot coshab - sinhab)coshay}{sinh2\alpha b + 2\alpha b} - \\ -\frac{\alpha y sinhay sinh\alpha b}{sinh2\alpha b + 2\alpha b}. \quad (10)$$

For square specimen, *a* is equal to *b* and $\varphi(y/b)$ can be described as:

$$\varphi(y/b) = \sum_{m=1}^{\infty}\left[\frac{(m\pi coshm\pi - \sin h\, m\pi)coshm\pi\frac{y}{b}}{sinh2m\pi + 2m\pi} - \right. \\ \left. -\frac{m\pi\frac{y}{b}sinh\frac{y}{b}sinhm\pi}{sinh2m\pi + 2m\pi}\right]. \quad (11)$$

For different positions on the *y* axis, $\varphi(y/b)$ can be approximation calculated according to Eq. (7). But the convergence times of the shape function is increased with the increase of *y/b*. The maximum tolerance is 1E-8 and the maximum number of convergence is 30 which have been listed in Table 1. The calculated results are also in agreement with the finite simulation results [14]. The expression of $\varphi(y/b)$ can be fitted as:

$$\varphi(y/b) = 0.625(y/b)^6 - 1.245(y/b)^5 + 0.913(y/b)^4 - \\ -0.313(y/b)^3 + 0.225(y/b)^2 - 0.002(y/b) + 0.101. \quad (12)$$

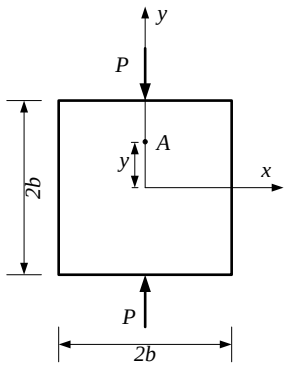

Fig. 2 Schematic diagram of the coordinate system of the square specimen under splitting load

Table 1

Calculation results of the shape factor

y/b	$\varphi(y/b)$
0	0.1013
0.1	0.1031
0.2	0.1085
0.3	0.1173
0.4	0.1297
0.5	0.1454
0.6	0.1643
0.7	0.1865

A specimen of rock-like material produced by white cement was introduced to verify the correctness of the formula. As shown in Fig. 3, the strain gauge $\varepsilon 1 \sim \varepsilon 5$ was fixed on the vertical symmetry axis of the specimen surface to test the tensile stress during the process of splitting loading.

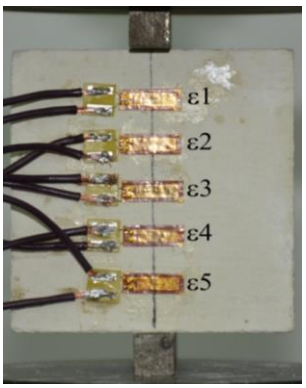

Fig. 3 Schematic diagram of the strain test

It can be seen from Fig. 4 that the tensile strain approximation increases linearly with the increase of the load. The maximum tensile stains are the strain gauge $\varepsilon 1$ and $\varepsilon 5$ and the minimum strain occurs at the center position, $\varepsilon 3$, as shown in Fig. 4, a. The difference between $\varepsilon 1$, $\varepsilon 5$ and $\varepsilon 3$ gradually increase with the increase of load. And then the stain of $\varepsilon 1$ reaches its peak value and the crack is initiated from $\varepsilon 1$ and then extend to other strain gauges. The theoretical stress at different locations can be obtained according to the Eq. (7). The elastic modulus, *E*, and Poisson ratio, μ, of this kind of rock-like material were determined by experiments as *E*=4.68 GPa and μ=0.22. Based on the stress and strain formula, the measured stress value can be obtained and the comparison results between the measured value and

theoretical value are plotted out in Fig. 4, b. It can be indicated that the theoretical value and the measured value are in agreement with the variation of the load.

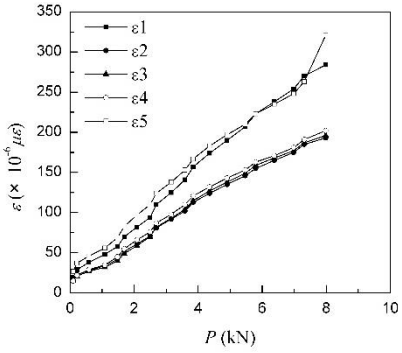

a

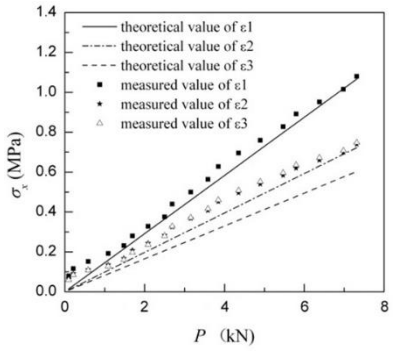

b

Fig. 4 Strain distribution: a - measured value; b - comparison of the measured value and theoretical value

3. The stress intensity factor of CSTSS

The stress intensity factor (SIF) is an important index of brittle fracture which can consider the singularity of the crack tip stress and effectively reflect the strength of the elastic stress field of the crack tip [15-16]. There is a lot of traditional solution of SIF, such as stress function method, integral transform method, finite element method, boundary element method, and boundary collocation method, whose computational accuracy is limited by the number of units. Similar to the domain integral method for J-Integral evaluation, the interaction integral method for stress-intensity factors calculation applies area integration for 2-D problems and volume integration for 3-D problems. In comparison to the traditional displacement extrapolation method, the interaction integral method offers better accuracy, fewer mesh requirements, and ease of use [17-20].

3.1. Calculation of stress intensity factor based on interaction integral method

An auxiliary field of the crack tip is established to separate and obtain the Mode I and the Mode II stress intensity factor in the real field for the interaction integral method. Around the crack tip, the auxiliary field must satisfy the equilibrium conditions, the physical equations and the geometric relationship of any possible displacement field and stress field [21].

The interaction integral is defined as:

$$I = -\int_V q_{i,j}\left(\sigma_{ki}\varepsilon_{ki}^{aux}\delta ij - \sigma_{kj}^{aux}u_{k,i} - \sigma_{kj}u_{k,i}^{aux}\right)dV \Big/ \Big/ \int_S \delta q_n dS, \quad (13)$$

where: σ_{ki}, σ_{kj}, u_{ki} are the stress, strain and displacement, σ_{kj}^{aux}, $u_{k,i}^{aux}$ are the stress, strain and displacement of the auxiliary field, $q_{i,j}$ is the crack-extension vector, The interaction integral is associated with the stress-intensity factors as:

$$I = \frac{2}{E^*}\left(K_I K_I^{aux} + K_{II}K_{II}^{aux}\right) + \frac{1}{G}K_{III}K_{III}^{aux}, \quad (14)$$

where: K_I, K_{II}, K_{III} are Mode I, II, and III stress intensity factors, K_I^{aux}, K_{II}^{aux}, K_{III}^{aux} are auxiliary Mode I, II and III stress intensity factors, $E^*=E$ for plane stress and $E^*=E/(1-\mu^2)$ for plane strain, E is Young's modulus, μ is Poisson's ratio, G is shear modulus.

For the plane problem, K_{III} can be ignored. Two auxiliary field conditions are $K_I^{aux}=1$, $K_{II}^{aux}=0$ and $K_I^{aux}=0$, $K_{II}^{aux}=1$, respectively. The Mode I and Mode II stress intensity factors can be obtained through the two interaction integral calculation by Eq. (14):

$$K_I = \frac{E^*}{2}I_1, \quad K_{II} = \frac{E^*}{2}I_2. \quad (15)$$

3.2. Finite element calculation accuracy verification

A calculation example is introduced to verify the accuracy of the interaction integral method. As shown in Fig. 5, the specimen of the cracked rectangular block was taken a load of the tensile stress of 2 MPa. The application of boundary conditions and meshing are shown in Fig. 6. The width, *b*, half height, *h*, thickness, *t*, and edge crack length, *a*, are 20mm, 80mm, 3mm, and 8mm separately. The Young's modulus and Poisson's ratio are 201 GPa and 0.258 separately. The Mode I stress intensity factor can be determined as:

$$K_I = F\sigma\sqrt{\pi a}, \quad (16)$$

where:

$$F = 1.12 - 0.23(a/b) + 10.6(a/b)^2 - \\ -21.7(a/b)^3 + 30.4(a/b)^4. \quad (17)$$

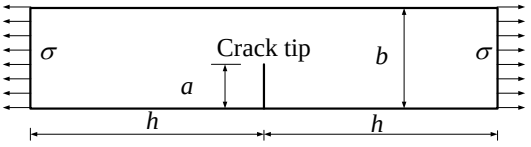

Fig. 5 Schematic diagram of a calculation example

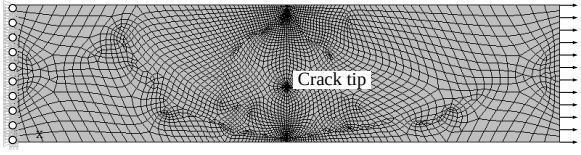

Fig. 6 Boundary conditions and mesh generation

The FEM results are compared with the exact solution of different crack lengths, which was listed in Table 2. It can be seen that the maximum error was about 0.646%. The interaction integral method can meet the requirement of engineering well.

Table 2

Accuracy validation results of calculation example

a, mm	a/b	K_I^{FEM}, MPa×m$^{1/2}$	$K_I^{[23]}$, MPa×m$^{1/2}$	Error, %
2	0.1	0.189	0.188	-0.403
4	0.2	0.307	0.308	0.423
6	0.3	0.456	0.457	0.339
8	0.4	0.669	0.670	0.107
10	0.5	1.001	1.008	0.646
12	0.6	1.566	1.573	0.451

3.3. Stress intensity factor calibration of CSTSS

A cracked straight through square specimen under splitting load with a thickness of t, a width of $2b$, a crack length of $2a$, shown in Fig. 7. The tensile stress of the same size uncracked specimen can be obtained by Eq. (9):

$$\sigma_x = \frac{2P}{bt}\varphi(a/b). \tag{18}$$

According to the general form of the Mode I stress intensity factor, the calculation formula for the Mode I fracture toughness, K_{IC}, of CSTSS can be expressed as:

$$K_{IC} = \sigma_x\sqrt{\pi a}\cdot F(a/b) = \frac{2P_M}{bt}\sqrt{\pi a}\varphi(a/b)F(a/b), \tag{19}$$

where: P_M is peak load and $F(a/b)$ is shape factor which can be calibrated by FEM.

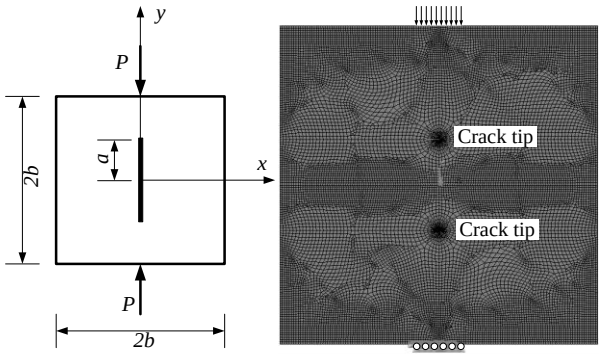

Fig. 7 Boundary conditions and mesh generation of CSTSS

The calibrated results of $F(a/b)$ through ANSYS interaction integral method was listed in Table 3. The shape factor, $F(a/b)$, decrease with the increase of a/b (Fig. 8). The formula of $F(a/b)$ can be obtained by polynomial fitting:

$$F(a/b) = 0.868(a/b)^6 - 4.858(a/b)^5 + \\ +7.351(a/b)^4 - 4.415(a/b)^3 + 0.685(a/b)^2 - \\ -0.245(a/b) + 1.487. \tag{20}$$

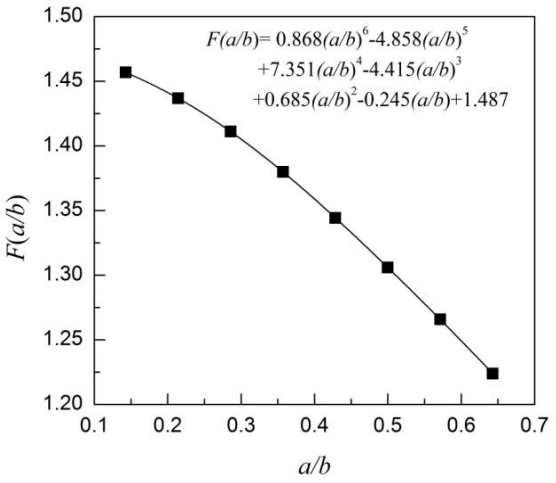

Fig. 8 Variation of shape factor

Table 3

Calibration result of stress intensity factor

a	a/b	$\varphi(y/b)$	K_I	$F(a/b)$
5.0	0.143	0.105	43.697	1.457
7.5	0.214	0.109	55.072	1.437
10.0	0.286	0.116	66.055	1.411
12.5	0.357	0.124	77.277	1.380
15.0	0.429	0.134	89.048	1.344
17.5	0.500	0.145	101.520	1.306
20.0	0.571	0.158	114.710	1.266
22.5	0.643	0.173	128.587	1.224

4. Test results

A specimen of rock-like material produced by white cement was introduced to test the Mode fracture toughness of CSTSS (Fig. 9). The specific specimen size was shown in Table 4. Displacement control was adopted in the experiment, and the loading rate was limited in 5 mm/min. The peak load was obtained after the experiment and substituted into the Eq. (13). The calculation results of K_{IC} was listed in Table 4. It was indicated that the values of K_{IC} were stabilized in relative range and the average value of K_{IC} was 0.140MPa×m$^{1/2}$.

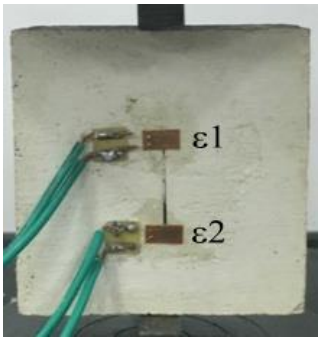

Fig. 9 Loading diagram of CSTSS

Table 4

K_{IC} test results of CSTSS

t, mm	P_M, kN	F, a/b	K_{IC} (MPa×m$^{1/2}$)
28.71	2.275	1.410154	0.130795
29.40	3.315	1.410154	0.186104
25.17	2.115	1.410154	0.138700
29.40	2.353	1.410154	0.132122
33.50	2.628	1.410154	0.129465
27.00	2.044	1.410154	0.124936

In order to verify the reliability of Mode I fracture toughness test method of the CSTSS, a three-point-bend fracture toughness test experiment of the same rock-like material was introduced as a comparison experiment (Fig. 10). The length, *L*, and the span, *S*, of the specimen are 250 and 200 mm separately.

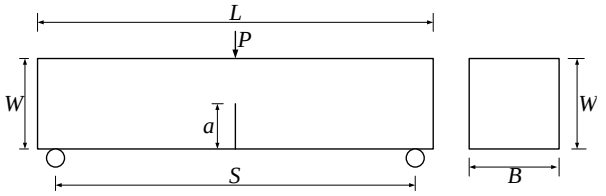

Fig. 10 Three-point-bend experiment

The Mode I fracture toughness of the three-point bending beam can be expressed as:

$$K_{IC} = F\frac{3SP_M}{2BW^2}\sqrt{\pi a}, \tag{21}$$

Where are P_M, *B*, *W* and *a* are peak load, length, height and crack length separately. *F* is shape factor and:

$$F = \frac{1.99 - \frac{a}{W}\left(1-\frac{a}{W}\right)\left[2.15 - 3.93\frac{a}{W} + 2.7\left(\frac{a}{W}\right)^2\right]}{\left[1+2\left(\frac{a}{W}\right)\right]\left(1-\frac{a}{W}\right)^{3/2}}. \tag{22}$$

The K_{IC} test results of the three-point-bend experiment were listed in Table 5. The average value of K_{IC} was about 0.158 MPa×m$^{1/2}$ which was slightly larger than that of CSTSS. It can be indicated through a comparison of Table 4 and Table 5 that the test results of K_{IC} by the two methods show a good agreement. Both the CSTSS and the three-point bend experiments are effective methods to determine the K_{IC} of rock.

Table 5

K_{IC} results of the three-point-bend experiment

W, mm	*B*, mm	P_M, N	*F*	K_{IC}, MPa×m$^{1/2}$
47	52	222	2.175	0.158237
46	51	239	2.210	0.184617
47	55	197	2.175	0.133195

5. Conclusions

1. Calculation formula of tensile stress of square specimen under splitting load was obtained through Fourier Series Solution of plane stress problems. And an experiment of testing strain was introduced to verify the correctness of the formula. The test results showed that the tensile strain approximation increases linearly with the increase of the load and the theoretical value and the measured value were in agreement with the variation of the load.

2. Based on the tensile stress distribution of the uncracked specimen and the general form of the Mode I stress intensity factor, the calculation formula of Mode I fracture toughness of cracked straight through the square specimen, CSTSS, under splitting load was obtained and the shape function was calibrated through finite element interaction integral method.

3. A rock-like material was used to produce CSTSS and three-point bend beam specimens. The Mode I fracture toughness K_{IC} was tested through CSTSS split experiment and three-point bend experiment. The average value of K_{IC} of the two different methods was well agreement. It was suggested that the CSTSS under splitting load can be a potential method to determine the Mode I fracture toughness of rock.

Acknowledgements

This research is supported by the National Key R&D Program of China (Grant No. 2016YFE0125600), the National Natural Science Foundation of China (Grant No. 51808509), the Foundation for University Key Teacher by the He'nan Educational Committee (Grant No. 2016GGJS-002).

References

1. **ISRM Testing Commission**. 1995. Suggested method for determining mode I fracture toughness using cracked chevron notched Brazilian disc (CCNBD) specimens, International Journal of Rock Mechanics & Mining Sciences & Geomechanics Abstracts 32: 57-64.
2. **Xu, Y.**; **Dai, F.**; **Zhao, T.**; **Xu, N.**; **Liu, Y.** 2016. Fracture toughness determination of cracked chevron notched brazilian disc rock specimen via griffith energy criterion incorporating realistic fracture profiles, Rock Mechanics and Rock Engineering 49: 3083–3093. https://doi.org/10.1007/s00603-016-0978-0.
3. **Wang, H.**; **Zhao, F.**; **Huang, Z.**; **Yao, Y.**; **Yuan, G.** 2017. Experimental study of Mode-I fracture toughness for layered shale based on two ISRM-suggested methods, Rock Mechanics and Rock Engineering 50: 1933-1939. https://doi.org/10.1007/s00603-017-1180-8.
4. **Wang, Q. Z.** 1998. Stress intensity factors of ISRM suggested CCNBD specimen used for mode-I fracture toughness determination, International Journal of Rock Mechanics & Mining Sciences 35: 977-982. https://doi.org/10.1016/S0148-9062(98)00010-2.
5. **Jia, X. M.; Wang, Q. Z.** 2003. Calibration of stress intensity factor for new type of fracture toughness specimen CCNBD suggested by ISRM. Chinese Journal of Rock Mechanics and Engineering 22: 1227-1233 (in Chinese).
6. **Wang, Q. Z.**; **Jia, X. M.** 2002. Determination of Elastic Modulus， Tensile Strength and Fracture Toughness of Brittle Rocks By Using Flattened Brazilian Disk Specimen--Part I: Analytical and Numerical Results. Chinese Journal of Rock Mechanics and Engineering 21: 1285-1289 (in Chinese).
7. **Elghazel, A.**; **Taktak, R.**; **Bouaziz, J.** 2015. Determination of elastic modulus, tensile strength and fracture toughness of bioceramics using the flattened Brazilian disc specimen: analytical and numerical results. Ceramics International 41:12340-12348. https://doi.org/10.1016/j.ceramint.2015.06.063.
8. **Wang, Q. Z.**; **Jia, X. M.**; **Kou, S. Q.**; **Zhang, Z. X.**; **Lindqvist, P. A.** 2004. The flattened Brazilian disc specimen used for testing elastic modulus, tensile strength and fracture toughness of brittle rocks: analytical and numerical results, International Journal of Rock Mechanics & Mining Sciences 41: 245-253.

https://doi.org/10.1016/j.ijrmms.2004.03.015.
9. **Dai, F.**; **Wei, M.D.**; **Xu, N. W.**; **Zhao, T.**; **Xu, Y.** 2015. Numerical investigation of the progressive fracture mechanisms of four ISRM-suggested specimens for determining the Mode I fracture toughness of rocks, Computers & Geotechnics 69: 424-441. https://doi.org/10.1016/j.compgeo.2015.06.011.
10. **Liang, Y. M.**; **Ke, X. J.**; **Hong, M. U.**; **Chun, H. H.** 2001. Approach to test method of rock strength in uniaxial tension, Journal of Guizhou University of technology (Natural Science) 30:19-25 (in Chinese).
11. **Garcia-Fernandez, C. C.**; **Gonzalez-Nicieza, C.**; **Alvarez-Fernandez, M. I.** 2018. Analytical and experimental study of failure onset during a Brazilian test, International Journal of Rock Mechanics and Mining Sciences 103: 254-265. https://doi.org/10.1016/j.ijrmms.2018.01.045.
12. **Yu, X. B.** 1991. Finite Element Method Analysis on Rock's Brzilian Test, Nonferrous Metals 43: 12-16.
13. **Wang, Z.** 2015. Test on Tensile Strength of Rectangular Rock Specimen, Chinese Journal of Underground Space and Engineering11: 370-374 (in Chinese).
14. **Wang, Z.**; **Zhang, J. F.**; **Du, Y. H.** 2014. Splitting Stress Analysis of Rock with Rectangular Shape, Science & Technology Revies 32: 39-43 (in Chinese).
15. **Chen, Z. Z.**; **Tokaji, K.** 2004. Effects of particle size on fatigue crack initiation and small crack growth in SIC particulate-reinforced aluminum alloy composites, Materials Letters 58: 2314-2321. https://doi.org/10.1016/S0167-577X(04)00153-3.
16. **Liu, X. Y.**; **Xiao, Q. Z.**; **Karihaloo, B. L.** 2004. XFEM for direct evaluation of mixed mode SIFs in homogeneous and bi-materials, International Journal for Numerical Methods in Engineering 59: 1103-1118. https://doi.org/10.1002/nme.906.
17. **Daimon**; **Ryutaro**; **Okada**; **Hiroshi.** 2014. Mixed-mode stress intensity factor evaluation by interaction integral method for quadratic tetrahedral finite element with correction terms, Engineering Fracture Mechanics 115: 22-42. https://doi.org/10.1016/j.engfracmech.2013.11.009.
18. **Chiaramonte Maurizio, M.**; **Shen, Y. X.**; **KeerMLeon, M.**; **Lew Adrian, J.** 2015. Computing stress intensity factors for curvilinear cracks, International Journal for Numerical Methods in Engineering 104: 260-296. https://doi.org/10.1002/nme.4938.
19. **Kim, J. H.**; **Paulino, G. H.** 2003. The interaction integral for fracture of orthotropic functionally graded materials: Evaluation of stress intensity factors, International Journal of Solids and Structures 40: 3967-4001. https://doi.org/10.1016/S0020-7683(03)00176-8.
20. **Amit, K. C.**; **Kim, J. H.** 2008. Interaction integrals for thermal fracture of functionally graded material, Engineering Fracture Mechanics 75: 2542-2565. https://doi.org/10.1016/j.engfracmech.2007.07.011.
21. **Gong, J. Q.**; **Zhang, S. Q.**; **Li, H.**; **Zhang, C. Y.** 2015. Computation of the Stress Intensity Factor Based on the Interaction Integral Method, Journal of Nanchang Hangkong University 29: 42-48 (in Chinese).

Lijuan ZHANG, Zhi WANG, Long LI

EXPERIMENTAL STUDY ON MODE I FRACTURE OF CRACKED STRAIGHT THROUGH THE SQUARE SPECIMEN (CSTSS)

S u m m a r y

Analytical solution of tensile stress of square specimen under splitting load was obtained through Fourier Series Solution of plane stress problems. According to the stress distribution of the un-cracked square specimen, the calculation formula of Mode I fracture toughness of cracked straight through the square specimen, CSTSS, under splitting load was obtained, and the shape function was corrected by the finite element interaction integration method. In order to verify the correctness of the formula, a CSTSS splitting test was performed. The test results indicated that the stress distribution on the axis of symmetry is consistent with the theoretical results, and the minimum tensile stress occurs at the center point of the un-cracked specimens. The Mode I fracture toughness of CSTSS, K_{IC}, was stabilized in relative range and the average value of K_{IC} was 0.140 MPa×m$^{1/2}$. The three-point-bend experiment was introduced as a comparative test and the average value of K_{IC} was 0.158 MPa×m$^{1/2}$ which was slightly larger than that of CSTSS. The test results indicated that both of the two tests could be reliable and the CSTSS under splitting load could be a potential method to determine the Mode I fracture toughness of rock.

Keywords: cracked straight through the square specimen (CSTSS), Model I fracture toughness, splitting load, finite element interaction integral method, rock-like materials.

Received March 16, 2019
Accepted February 03, 2020